HHS Public Access

Author manuscript

Nat Chem Biol. Author manuscript; available in PMC 2016 October 18.

Published in final edited form as:

Nat Chem Biol. 2016 June ; 12(6): 399–401. doi:10.1038/nchembio.2068.

Light-induced nuclear export reveals rapid dynamics of epigenetic modifications

Hayretin Yumerefendi[1], **Andrew Michael Lerner**[1], **Seth Parker Zimmerman**[1], **Klaus Hahn**[2,4], **James E Bear**[3,4], **Brian D. Strahl**[1,4], and **Brian Kuhlman**[1,4]

[1]Department of Biochemistry and Biophysics, University of North Carolina, Chapel Hill, North Carolina 27599, USA

[2]Department of Pharmacology, University of North Carolina, Chapel Hill, North Carolina 27599, USA

[3]Department of Cell Biology & Physiology, University of North Carolina, Chapel Hill, North Carolina 27599, USA

[4]Lineberger Comprehensive Cancer Center, University of North Carolina, Chapel Hill, North Carolina 27599, USA

Abstract

We engineered a photoactivatable system for rapidly and reversibly exporting proteins from the nucleus by embedding a nuclear export signal in the LOV2 domain from phototropin 1. Fusing the chromatin modifier Bre1 to the photoswitch, we achieved light-dependent control of histone H2B monoubiquitylation in yeast, revealing fast turnover of the ubiquitin mark. Moreover, this inducible system allowed us to dynamically monitor the status of epigenetic modifications dependent on H2B ubiquitylation.

Light-sensitive proteins are powerful tools for interrogating biological phenomena because they can be manipulated with precise control in space and time[1]. One generalizable approach for regulating the activity of a protein is to control its cellular localization[2,3]. We and others recently demonstrated that the photosensitive LOV2 domain from *Avena sativa* phototropin 1 (AsLOV2) can be used to photocage a nuclear localization signal (NLS) so that the protein localizes to the nucleus when AsLOV2 is stimulated with blue light[4,5]. Here, we demonstrate a complementary strategy for controlling nuclear export to rapidly eject a protein from the nucleus.

Correspondence to: bkuhlman@email.unc.edu.

Author Contributions

HY and BK conceived the project and designed the experiments. HY, AML and SPZ performed the experiments. HY, AML, SPZ, BDS and BK analyzed the results. KH and JEB provided reagents and equipment. HY and BK wrote the manuscript with input from all authors.

Addgene Accession IDs

73614-8 (see supplementary Table 4)

Competing financial interests

The authors declare no competing financial interests.

Upon blue light stimulation, the AsLOV2 domain undergoes a conformational change that results in the unfolding of its N-terminal (A′α helix) and C-terminal helices (Jα helix)[6,7]. To create photoinducible nuclear export, we embedded a nuclear export signal (NES) in the Jα helix so that it is sterically blocked from binding to its natural binding partner, the major nuclear export receptor CRM1[8], in the dark, but accessible upon light illumination (Fig. 1a). We used established amino acid preferences for NES motifs to guide the design using a previously engineered sequence, the Super-PKI-2 motif, as our starting point[9]. We positioned the Super-PKI-2 motif within the Jα helix in a manner that maximized sequence conservation with the wild-type AsLOV2 sequence (Fig. 1a). Additionally, we explored an alternative strategy based on creating a single contiguous helix joining two AsLOV2 domains (Fig. 1b and Supplementary Results, Supplementary Fig. 1). In this approach, the designed NES starts at the C-terminus of the Jα helix and continues into a second copy of AsLOV2, replacing its A′α helix. Because the NES sequence is embedded in a different structural environment with this alternative strategy, we adjusted its sequence to maintain the integrity of the A′α and Jα helices. To direct the switches to the nucleus in the dark, we fused the AsLOV2/NES chimeras to an NLS. This allows the nucleocytoplasmic distribution of the switch to be tuned by incorporating NLSs of varying import efficiencies[10] (Supplementary Fig. 2, Supplementary Table 1). The resultant switch we named Light Inducible Nuclear eXporter (LINX). The two flavors of designs, a single AsLOV2 domain versus two AsLOV2 domains, are referred to as LINXa and LINXb followed by a number denoting the NLS sequence used.

We first evaluated the switches coupled to NLS3 in mouse fibroblasts (IA32) expressing them as fusions with fluorescent proteins and monitoring nucleocytoplasmic ratios upon blue light exposure with confocal microscopy. Both LINXa and LINXb were able to reversibly direct protein in and out of the nucleus. (Fig. 1c, Supplementary Movie 1, 2, 3 and 4). LINXa produced a 4-fold change in nucleocytoplasmic ratio while LINXb exhibited a smaller change (2.3-fold), but had lower nuclear protein levels in the light than LINXa (Fig. 1c and 1d, Supplementary Movie 1 and 2, Supplementary Table 2). Neighboring, unstimulated cells were unaffected (Fig 1c and Supplementary Fig. 3) and multiple cells could be simultaneously activated without large cell-to-cell variability (Supplementary Fig. 4). We also tested LINXa in yeast and in *C. elegans*. (Supplementary Fig. 5, 6 and Supplementary Movie 5). Export kinetics were rapid in all systems, with half-lives of 5 seconds in *C. elegans*, 8 seconds in yeast, and 68 seconds in mouse fibroblast cells. The half-lives for import, which are partially dictated by the ~30 second lit to dark reversion time of the AsLOV2 domain, ranged from 38 seconds in yeast to 3.8 minutes in fibroblasts (Supplementary Fig. 7).

To better understand the relative activities of LINXa and LINXb, we characterized a set of mutations in their NES motifs (Supplementary Fig. 8, Supplementary Table 2). In general, NES mutations that disrupted buried contacts in the dark state of LINXa or LINXb lowered the fold change in nucleocytoplasmic ratio upon light activation. The lower levels of nuclear protein for LINXb can be partially explained by the use of a leucine in the Φ_1 position of the NES motif, which provides optimal binding to CRM1[9]. We also observed that both domains of AsLOV2 are required to make LINXb an effective switch (Supplementary Fig. 1, 5 and Supplementary Table 2).

We then explored whether the capabilities of LINX could be extended by using it with the iLID system[11], which forms a heterodimer when activated with blue light (Fig. 1e). By fusing one half of the dimer to the mitochondria and the other to LINXa we were able to relocate the protein from the nucleus to the mitochondria with light (Fig. 1f and Supplementary Fig. 9, Supplementary Movie 6). Nuclear levels of LINXa in the light were reduced relative to using LINXa alone, providing a strategy for further reduction of nuclear protein activity.

To demonstrate control of protein function with LINX, we first used it to regulate the activity of a transcription factor in yeast. We fused the LexA DNA binding domain and the Gal4 activation domain to LINXa and LINXb, and coupled them with NLS signals of decreasing strength[12] (NLS3, NLS4 and NLS5) (Fig. 2a, Supplementary Table 1). These constructs were tested in the yeast strain NMY51 (Supplementary Table 3) that has a LexA binding site upstream of the *lacZ* gene, which encodes β-galactosidase. Lower levels of β-galactosidase activity were observed for both switches in the light, and consistent with the microscopy results, LINXb was less active than LINXa when using the same NLS. The largest change in activity, 15-fold, was observed with LINXa4. We also used iLID to direct the LINXa3-nano/transcription factor fusion to the plasma membrane and observed 8-fold lower β-galactosidase activity in the light compared to LINXa3 alone, which was accompanied by equally lower activity in the dark (Fig. 2b).

We next tested if LINX could be used to control a chromatin modifier. Epigenetic signaling is a dynamic process that regulates gene transcription through post-translational modifications to histones and DNA, and has not previously been interrogated with light-activatable switches. Bre1 is an E3 ubiquitin ligase that monoubiquitylates K123 on histone H2B (H2Bub1) and promotes transcriptional activation and elongation by RNA polymerase II[13]. Previous experiments relying on chemical perturbations have shown that H2BK123 is dynamically ubiquitylated and deubiquitylated on timescales faster than 30 minutes, but have not provided sufficient temporal resolution to precisely measure these rates and subsequent events[14,15]. We silenced a putative NLS in Bre1[16] between amino acids 5-13 by mutating all of the lysines in the motif to alanines and tested if we could constitutively inactivate Bre1 by fusing it to the NES signal from LINXa. Expression of this construct in a *bre1* deletion strain (*bre1Δ,* Supplementary Table 3) resulted in a complete loss of H2Bub1 (Fig. 2c). We then expressed the C-terminally fused NLS-silenced Bre1 to LINXa4 and probed for H2Bub1 after 5 hours of light or dark treatment. H2Bub1 was reduced in the lit sample, accompanied by lower levels of histone H3K4 trimethylation (H3K4me3) and histone H3K79 trimethylation (H3K79me3). H3K4me3 and H3K79me3 are known to be dependent on *trans*-histone regulation by H2Bub1[17,18]. Conversely, H3K36me3 was not affected by nuclear removal of Bre1, as expected since this modification is regulated independently from H2Bub1. We also coupled iLID with LINXa4-Bre1 and observed a further loss of H2Bub1 in the light and additional loss of H3K79me2 and H3K4me3. To confirm that changes in H2Bub1 levels were due to changes in Bre1 localization, we fused mVenus to LINXa4-Bre1 and performed microscopy in yeast (Supplementary Table 3). Light stimulation reduced nucleocytoplasmic ratios ~3-fold with an export $t_{1/2}$ of 28 seconds and import $t_{1/2}$ of 6.4 minutes (Supplementary Fig. 10 and Supplementary Movie 7).

To measure turnover rates for global levels of H2Bub1, we maintained Bre1-LINXa4-expressing yeast in lit or dark conditions for 4 hours, reversed the conditions, and probed H2Bub1 levels at time points over one hour. For the dark to light transition, we observed rapid removal of H2Bub1 to steady state levels with a $t_{1/2}$ of 1.1 minutes, followed by removal of H3K4me3 ($t_{1/2}$ = 15 mins) (Fig. 2d and Supplementary Fig. 11a). The lag in H3K4me3 removal corroborates the observation that Jhd2, the H3K4 demethylase, requires the removal of H2Bub1 in order to recognize its target[19]. H3K79me3 levels persisted throughout the one-hour time course, which further supports the hypothesis that H3K79me3 is lost passively[20]. Significantly, the lit to dark transition allowed us to also probe the appearance of these epigenetic marks (Fig. 2e and Supplementary Fig. 11b). H2Bub1 appeared and came to a steady state level with a $t_{1/2}$ of 6.3 minutes, which was accompanied by H3K4me3 with a $t_{1/2}$ of 17.4 minutes. Unexpectedly, the buildup of H3K79me3 was noticeably slower. Global levels of LINXa4-Bre1 remained steady throughout both time courses (Supplementary Fig. 11c and d). In both time courses the rates we measured for ubiquitin placement and removal are similar to the rates of import and export we measured via microscopy for the LINXa4-Bre1 switch, which suggests that H2B ubiquitylation and deubiquitylation may occur at rates that are even faster than can be detected with our current approach. This demonstrates the rapid nature of chromatin remodeling and the requirement for tools to accurately probe its kinetics. Our results also indicate that the mechanistic pathways leading to H3K4me3 and H3K79me3 are distinct, and suggest that re-establishment of H3K79me3 by the methyltransferase Dot1 occurs via a mechanism that goes beyond the simple re-establishment of H2Bub1, and thus likely involves secondary events[19].

In conclusion, we have engineered a versatile and tunable suite of photoswitches for the control of nuclear export with blue light, which allows for the regulation of transcription factors and epigenetic modifiers. Additionally, the coupling of LINX with iLID or other light inducible dimers should be useful for studying proteins that exhibit distinctive functions in the nucleus and the PM or other subcellular locations.

Online Methods

Reagents

Immunoblots were developed using ECL Prime (Amersham RPN2232). Antibodies: H2B K123Ubq1 (Cell Signaling Technologies 5546; 1:1,000), H2B (Active Motif 39237; 1:5,000), H3K79me3 (Abcam 2621; 1:2,000), H3K79me2 (Active Motif 39143; 1:2,500), H3K4me3 (Epicypher 13-0004; 1:5,000), H3K36me3 (Abcam 9050; 1:1,000), H3 (Epicypher 13-0001; 1:5,000), G6PDH (Sigma Aldrich A9521; 1:100,000), FLAG (Sigma Aldrich F7425; 1:1,000). Rabbit (Amersham NA934; Donkey anti-Rabbit) and mouse (Amersham NA931; Sheep anti-mouse) secondary antibodies were used at 1:10,000.

C. elegans strain construction and microscopy

All strains were maintained at 20°C or 25°C on NGM medium, using *E. coli* strain OP50 as a food source. To express mKate2::LINXa3 in MS cells, a construct carrying the mKate2::LINXa3 coding sequence was cloned into a modified pCFJ151 containing the

ceh-51 promoter and *tbb-2* 3'UTR. This construct was injected into wild type worms (strain N2) to generate extrachromosomal arrays. Embryos expressing mKate2::LINXa3 were mounted on polylysine-coated coverslips and gently flattened using 2.5% agar pads. For whole-embryo photoactivation experiments we used an Olympus DSU-IX81 Spinning Disk Confocal equipped with a 100X, UPLFLN objective. The microscope was coupled with Andor solid-state lasers (Andor) and controlled using Metamorph (Molecular Devices). Confocal images of mKate2 fluorescence were captured every 2-3 s, and the embryos were illuminated with blue light from a 488 nm laser for 1s between each pair of image acquisitions (5% laser power).

Mammalian cell culture, transfection and microscopy

Mouse IA32 fibroblasts were generated in-house [1]. This cell line was chosen for mammalian studies because of its morphological characteristics. The cell body is well spread which allowed us to easily distinguish the cytoplasm from the nucleus.

LINXa constructs were cloned via overlap extension PCR. During the PCR a Nuclear Localization Sequence (NLS) and a KpnI restriction site were added to the 5' end and a BamHI restriction site was added between the NLS and AsLOV2 domain. A similar strategy was used to add the conditional NES at the 3' end along with a HindIII site. Subsequently, restriction digests were performed with KpnI and HindIII to introduce the LINX construct into a pTriEx vector[5]. For LINXb, LINXa was used as a template to add the cNES at the 3' end and introduce a SacI restriction site (encoding residues EL) at the end of the cNES between Φ_3 and Φ_4, thus generating the first copy of AsLOV2 without sequence scarring. For the second copy of AsLOV2 in LINXb, LINXa was similarly used as a template introducing a SacI restriction site at its 5' end and a HindIII site at its 3' end. The two PCR fragments were digested with BamHI and SacI or SacI and HindIII respectively, and cloned into a LINXa plasmid harboring the respective NLS by three-parts ligation. Please refer to supplementary protein sequences for complete sequence details of the constructs.

Cells were transfected with the appropriate vector containing the sequence encoding the LINX of interest [2]. After 24 hours the transfected cells were trypsonized and transferred to 3.5 cm MatTek glass bottom dishes coated with a 10 μg/ml solution of fibronectin. 24 – 48 hours later cells were imaged and photo-activated with an Olympus FV1000 confocal microscope equipped with a 1.30 N.A. 40x oil immersion objective. The Time Controller module found in the Olympus Fluoview software was used to produce a timeline of image acquisition and photo-activation. Image acquisition used the 514 nm or 559 nm laser line dependent on the fluorophore (Venus or mCherry). At each image acquisition 3 optical sections were acquired. Each section contains an 800×800 image. Before activation images were taken every 7 sec. During activation images were taken every 47 seconds with the activation sequence in between each acquisition step. After activation images were acquired every 10 sec. The activation sequence consisted of rastorizing 250 × 250 pixels with 1% of the 488 nm laser and a pixel dwell time of 8 μs/pixel. Acquisition and Activation parameters were kept constant between samples.

HeLa and Cos7 (ATCC) were deemed appropriate as commonly used cells for nucleaocytoplasmic distribution of proteins of interest. Coverslips were washed with PBS

(GIBCO) and coated with 10 μg/ml fibronectin at room temperature for a minimum of 1.5 hours. Cells were seeded for a minimum of 3 hours to overnight, then transfected using FuGENE 6 (Promega), incubated for ~18 hours, and imaged in Ham's F-12K medium free of Phenol red (Caisson) containing 10 % FBS buffered with 10 mM HEPES pH 8. Coverslips were mounted in an Attofluor live cell chamber (Invitrogen) and placed in a microscope stage with a heated stage adaptor (Warner) and an objective temperature controller (Bioptechs).

An Olympus DSU-IX81 Spinning Disk Confocal coupled with Andor solid-state lasers (Andor) was used to perform the nuclear export signal screen. Z-stacks of 12 μm at 0.5 μm steps were acquired with a PlanApo 60× objective (Oil, N.A. 1.42) using a 561 nm laser set at 20% intensity (150 EM gain and 300 ms exposure).

Alternatively, an Olympus IX81 epifluorescence microscope equipped with a ZDC focus drift compensator and a Photometrics CoolSnap ES2 CCD camera (Roper Photometrics) was used with a UPlanFLN 40× objective (Oil, N.A. 1.30) and an ET572/35x filter for mCherry detection and 1% neutral density filter (UVND 2.0, ET430/24x).

Yeast Microscopy

MBP was substituted with mVenus in LINXa3-nano and LINXb3 yeast transcription clones in pNIA-CEN-MBP by generating two inserts: LexA with HindIII restriction site at its 5' and XbaI at its 3' and mVenus with XbaI and NotI respectively. pNIA-CEN-MBP was cut with HindIII and NotI and three piece ligation was performed to insert LexA and mVenus instead. Venus-FLAG-LINXa4-Bre1 was generated by cutting FLAG-LINXa4-Bre1 with HpaI, followed by dephosphorylation with Antartic Phosphatase. mVenus was amplified with forward and reverse primer that harbor XbaI restriction sites. The insert was digest with XbaI and polished by Pfu polymerase. Finally, it was blunt-end ligated into the previously generated backbone. The resultant plasmids were transformed via high efficiency lithium acetate transformation in H2B-mCherry yeast strain (gift from Kerry Bloom) and plated on SC-Leu dropout agar plates.

Single colonies were isolated and grown in 5 mL SC-Leu overnight. On The next day they were diluted to OD_{600} = 0.3 and grown for about 4 hours to OD_{600} ~ 1. About 20 μL of culture was then pipetted onto SC-Leu agar and covered with a coverslip. The samples were imaged with and photo-activated with an Olympus FV1000 confocal microscope equipped with a 100x (N.A. 1.40) oil immersion objective. The Time Controller module found in the Olympus Fluoview software was used to produce a timeline of image acquisition and photo-activation. Image acquisition used the 514 nm or 559 nm laser line. At each image acquisition a single optical section was acquired. A single image was taken before activation. During activation images were taken every 10 s with the activation sequence in between each acquisition step. After activation images were acquired every 30 s.

Image analysis and quantification

All images were analyzed using FIJI software. For each series of images, maximum intensity projections were produced of the 3 optical sections. For each cell of interest, elliptical regions of interest of the same size and shape were marked inside the nucleus and

just outside of the nucleus. The fluorescence intensity of these areas was measured throughout the image series. A ratio of nuclear to cytoplasmic fluorescence intensity was then calculated and plotted through time. The values that correspond to the period of activation and reversion were fit to the equations Y = (Y0 - Plateau)*exp(−K × X) + Plateau and Y = Ymax(1-e^{-kx}) respectively. Statistical analysis was performed using GraphPad Prism software. For experiments with Venus-iLID-Mito, the mitochondrial ROI was automatically selected by thresholding the Venus.

Yeast transcription

LINXa constructs were amplified from the previously generated mammalian vectors using overlap extension PCR to suppress BamHI present between the NLS and the LINX construct and add EcoRI at the 5' end and BamHI at the 3' end. Similarly, the pTriEx mammalian vectors, LINXb constructs were amplified in two pieces and three part ligations was performed using EcoRI and BamHI 5' end and 3' end respectively. Then, they were cloned into a pNIA-CEN-MBP plasmid[5] using EcoRI and BamHI restriction digest cloning downstream of the LexA DNA binding domain, MBP and Gal4AD. The resultant plasmid was transformed via high efficiency lithium acetate transformation in NMY51 yeast cells (gift from Chandra Tucker) and plated on SC-Leu dropout agar plates [3].

β-Galactosidase assays were performed as follows: Fresh colonies were grown overnight at 30°C in 5 ml SC-Leu. On the next day, the cell density was measured at OD_{600} and 2 mL cultures were diluted to OD_{600} = 0.2 in duplicates. Cultures were grown for 2 hours in the dark and then blue light of 500 μW/cm^2 (465 nm via LED strip light wrapped around the tube rack) was set to illuminate the lit set of the samples. The dark samples were wrapped in aluminium foil and grown in the same incubator. Cultures were grown at 30°C in a shaking incubator (250rpm) for another 4 hours. The resulting cultures were pelleted in triplicate and a β-Galactosidase assay using CPRG for a substrate was performed according to the manufacturer (Clontech).

Bre1 steady state light control

Bre1 was amplified from a plasmid (gift from Hashem Meriesh) with overlap extension PCR to mutate its predicted NLS by introducing three point mutations K8A, K9A and K11A and adding XmaI and BamHI restriction sites at its 5' and 3' respectively. LINXa4 was also amplified from pNIA-CEN-MBP vector used for transcriptional shutdown introducing XbaI and XmaI restriction sites at its 5' and 3' respectively. Finally, using a pNIA-CEN-MBP plasmid with an upstream FLAG-tag, the LINXa4 and *bre1* were sequentially cloned via restriction digest cloning. The resultant plasmid was transformed via high efficiency lithium acetate transformation in *bre1Δ* yeast cells (Open Biosystems) and plated on SC-Leu dropout agar plates.

Colonies were grown overnight at 30° C in the dark in SC-Leucine or SC-Leucine-Uracil. In the morning cell density was measured at OD_{600} and cultures were diluted in appropriate dropout media to a final volume of 6.5 mL and final OD_{600} of 0.3. LINX transformed cultures were diluted in duplicate, one of which was exposed to 500 μW/cm^2 blue light while the other was wrapped in foil and placed in the same incubator at 30° C. After 5 hours

of growth OD_{600} was again measured and 5 OD_{600} units of each asynchronous log phase culture were collected by centrifugation. Cells were subjected to glass bead lysis in SUMEB (1% SDS, 8 M urea, 10 mM MOPS, pH 6.8, 10 mM EDTA, 0.01% bromophenol blue) by vortexing at 4° C for 8 minutes. Extracts were retrieved and clarified by centrifugation and boiled at 95° C for 5 minutes. 10 μL of whole cell extract were loaded on 15% SDS-PAGE gels. Proteins were transferred to 0.45 μm PVDF membranes using a Hoefer Semi-Dry Transfer Apparatus at 45 mA per membrane. Primary antibodies were incubated in 5% milk at 4° C overnight and secondary antibodies were incubated in 5% milk for 1 hour.

Bre1 time courses

Colonies of LINXa4-Bre1 transformed in *bre1Δ* yeast strain were grown overnight at 30° C in the dark or 200 $\mu W/cm^2$ blue light in SC-Leucine. In the morning cell density was measured at OD_{600}, cultures were diluted to a final volume of 60 mL and final OD_{600} of 0.35. After 4 hours of growth in the same light conditions OD_{600} was again measured. Time-courses began when cultures were moved from dark to light (Panel D) or light to dark (Panel E). At each time point the same volume of each culture (5 OD_{600} units measured at time 0) was harvested and added to the appropriate volume of 100% TCA (Sigma, 100% w/v) to a final concentration of 20%, followed by vigorous mixing and immediate centrifugation at 5000 rpm. Supernatant was aspirated and pellets frozen at −80°C. After the completion of each time-course, cells were resuspended in 20% TCA and subjected to glass bead lysis by vortexing at 4° C for 8 minutes. Extracts were collected by centrifugation, beads were washed in 5% TCA and precipitant was collected by centrifugation. Precipitated proteins were washed with 100% ethanol and solubilized in 1 M Tris HCl pH 8.0. Extracts were diluted in SDS-PAGE loading buffer (60 mM Tris pH 6.8, 2% SDS, 10% glycerol, 100 mM DTT, 0.2% bromophenol blue) and boiled at 95° C. Gel loads were normalized by applying a linear fit to OD_{600} measured before T_0 and immediately after T_{60}.

Western blot quantification

Data for band intensities for G6PDH for each gel, FLAG, H2B, H2Bub1, H3, H3K4me3 and H3K79me3 was extracted using ImageJ with an additional field for background. Background was subtracted from each. In the case of H2Bub1 the normalization against H2B was performed by directly dividing the H2Bub1 signal by the H2B signal for each respective time point since they came from the same protein gel (H2Bub1 runs at about 25 kDa and H2B – a little above 15 kDa). In the case of H3K4me3 and H3K79me3, which co-migrate with H3, different protein gels were used to probe for H3, H3K4me3 and H3K79me3. Therefore, H3K4me3, H3K79me3, and H3 were first normalized against G6PDH (present in each gel and lane), before normalizing H3K4me3 and H3K79me3 against H3 levels. Finally, to obtain relative abundance throughout the dark to light time course the first time point was used as a reference for each subsequent time point and respectively in the case of light to dark time course the last time point was used as a reference. The relative abundance values for H2Bub1, H3K4me3 and H3K79me3 were plotted using GraphPad Prism 5. The data were fit using single exponentials to obtain half-lives.

Protein expression

The *Avena sativa* phototropin-1 gene corresponding to residues 404-546 encoding for the LOV2 domain was amplified with two-step overlap extension PCR in order to introduce the designed nuclear localization signal, and then cloned into the vector pQE-80L at the BamHI and HindIII restriction sites. The resulting plasmid was transformed in BL21 (DE3) pLysS and bacteria were grown in 1.5 L Luria Bertani media until the culture reached OD_{600} ~ 0.6 at which point protein production was induced with 500 mM IPTG overnight (18-20h) at 25°C. Cell pellets were resuspended in 50 mM Tris pH 7.5, 1 M NaCl, 10 mM Imidazole, 10 mM β-ME and 1 mM PMSF and lysed using a cell disruptor. Lysed cells were then centrifuged for 30 min at 18564 RCF, then the supernatant was filtered through a 5 μM filter and loaded on 5 mL HisTrap IMAC columns (GE Healthcare). The columns were washed with 25 CV of 50 mM Tris pH 7.5, 1 M NaCl, 10 mM Imidazole, 10 mM β-ME and eluted on BioLogic LP (BioRad) using a gradient against 50 mM Tris pH 7.5, 100 mM NaCl, 500 mM Imidazole, 10 mM β-ME. The eluted protein was concentrated with Amicon Ultra-15 (Millipore) to 2 mL and subjected to size exclusion chromatography in 50 mM Tris pH 7.5, 100 mM NaCl and 1 mM DTT with HiLoad 16/600 Superdex 75 (GE Healthcare) run on an Akta FPLC (Amersham). The protein was extensively dialyzed sequentially against two times 4 L of 50 mM 100 mM NaCl Tris pH 7.5. Then, the protein was concentrated to 1 mL using Amicon Ultra-15 (Millipore) concentrators. Finally, the protein concentration was determined using a BCA assay following the manufacturer's protocol (Thermo Scientific Pierce).

Thermal reversion

Thermal reversion kinetics were determined with 20 μM of purified LINXa in 1.1 mL of 50 mM Tris pH7.5, 100 mM NaCl and 1mM DTT after illumination for 2 min with blue light (455nm, 6.0 mW/cm^2) at room temperature. Absorption measurements were taken immediately after the illumination for every 5 nm between 500-400 nm (speed 4800 nm/min) using a Cary 50 UV-Vis spectrometer (Varion). The absorbance was collected continuously for 5 minutes. The procedure was repeated 3 times.

Statistical analysis

Data is shown as mean ± s.e.m., with sample numbers indicated in figure legends. Microscopy images and western blots are representative from at least three experiments. To combine replicate experiments in Figure 3e and 3g data normalization was performed to account for the variation in sample loading as described in the Western blot quantification section above. The number of replicates was deemed appropriate as the s.e.m. from our replicates were smaller than the difference in mean values that we were comparing. Statistical significance was determined by two-tailed t-tests for the results in Figure 1a and 1b. All fits and statistical analysis were performed with GraphPad Prism 5.

Supplementary Material

Refer to Web version on PubMed Central for supplementary material.

Acknowledgements

We would like to thank Daniel Dickinson for help with *C. elegans* injections, Hashem Meriesh for providing a plasmid containing Bre1 and Raghuvar Dronamraju and Zu-Wen Sun for helpful discussions.

Funding: JEB (NIH GM111557), BK, KH, BS (NIH DA036877), KH (GM102924)

References

1. Tischer D, Weiner OD. Illuminating cell signalling with optogenetic tools. Nat Rev Mol Cell Biol. 2014; 15:551–558. [PubMed: 25027655]
2. Yang X, Jost AP-T, Weiner OD, Tang C. A light-inducible organelle-targeting system for dynamically activating and inactivating signaling in budding yeast. Molecular Biology of the Cell. 2013; 24:2419–2430. [PubMed: 23761071]
3. Gautier A, et al. Genetically encoded photocontrol of protein localization in mammalian cells. J Am Chem Soc. 2010; 132:4086–4088. [PubMed: 20218600]
4. Yumerefendi H, et al. Control of Protein Activity and Cell Fate Specification via Light-Mediated Nuclear Translocation. PLoS ONE. 2015; 10:e0128443. [PubMed: 26083500]
5. Niopek D, et al. Engineering light-inducible nuclear localization signals for precise spatiotemporal control of protein dynamics in living cells. Nat Comms. 2014; 5:4404.
6. Harper SM, Harper SM, Neil LC, Gardner KH. Structural Basis of a Phototropin Light Switch. Science. 2003; 301:1541–1544. [PubMed: 12970567]
7. Zayner JP, Antoniou C, Sosnick TR. The amino-terminal helix modulates light-activated conformational changes in AsLOV2. Journal of Molecular Biology. 2012; 419:61–74. [PubMed: 22406525]
8. Hutten S, Kehlenbach RH. CRM1-mediated nuclear export: to the pore and beyond. Trends Cell Biol. 2007; 17:193–201. [PubMed: 17317185]
9. Güttler T, et al. NES consensus redefined by structures of PKI-type and Rev-type nuclear export signals bound to CRM1. Nat Struct Mol Biol. 2010; 17:1367–1376. [PubMed: 20972448]
10. Hodel MR, Corbett AH, Hodel AE. Dissection of a nuclear localization signal. J Biol Chem. 2001; 276:1317–1325. [PubMed: 11038364]
11. Guntas G, et al. Engineering an improved light-induced dimer (iLID) for controlling the localization and activity of signaling proteins. P Natl Acad Sci Usa. 2015; 112:112–117.
12. Hodel AE, et al. Nuclear localization signal receptor affinity correlates with in vivo localization in Saccharomyces cerevisiae. J. Biol. Chem. 2006; 281:23545–23556. [PubMed: 16785238]
13. Xiao T, et al. Histone H2B ubiquitylation is associated with elongating RNA polymerase II. Molecular and Cellular Biology. 2005; 25:637–651. [PubMed: 15632065]
14. Fuchs G, Hollander D, Voichek Y, Ast G, Oren M. Cotranscriptional histone H2B monoubiquitylation is tightly coupled with RNA polymerase II elongation rate. Genome Res. 2014; 24:1572–1583. [PubMed: 25049226]
15. Henry KW, et al. Transcriptional activation via sequential histone H2B ubiquitylation and deubiquitylation, mediated by SAGA-associated Ubp8. Genes & Development. 2003; 17:2648–2663. [PubMed: 14563679]
16. Kosugi S, Hasebe M, Tomita M, Yanagawa H. Systematic identification of cell cycle-dependent yeast nucleocytoplasmic shuttling proteins by prediction of composite motifs. P Natl Acad Sci Usa. 2009; 106:10171–10176.
17. Sun Z-W, Allis CD. Ubiquitination of histone H2B regulates H3 methylation and gene silencing in yeast. Nature. 2002; 418:104–108. [PubMed: 12077605]
18. Briggs SD, et al. Gene silencing: trans-histone regulatory pathway in chromatin. Nature. 2002; 418:498–498. [PubMed: 12152067]
19. Huang F, et al. Interaction of the Jhd2 H3K4 demethylase with chromatin is controlled by histone H2A surfaces and restricted by H2B ubiquitination. J Biol Chem. 2015 jbc.M115.693085 doi: 10.1074/jbc.M115.693085.

20. Katan-Khaykovich Y, Struhl K. Heterochromatin formation involves changes in histone modifications over multiple cell generations. The EMBO Journal. 2005; 24:2138–2149. [PubMed: 15920479]

21. Cai L, Makhov AM, Schafer DA, Bear JE. Coronin 1B antagonizes cortactin and remodels Arp2/3-containing actin branches in lamellipodia. Cell. 2008; 134:828–842. [PubMed: 18775315]

22. Hallett RA, Zimmerman SP, Yumerefendi H, Bear JE, Kuhlman B. Correlating in Vitro and in Vivo Activities of Light-Inducible Dimers: A Cellular Optogenetics Guide. ACS Synth Biol. 2016; 5:53–64. [PubMed: 26474029]

23. Gietz RD, Schiestl RH. Quick and easy yeast transformation using the LiAc/SS carrier DNA/PEG method. Nat Protoc. 2007; 2:35–37. [PubMed: 17401335]

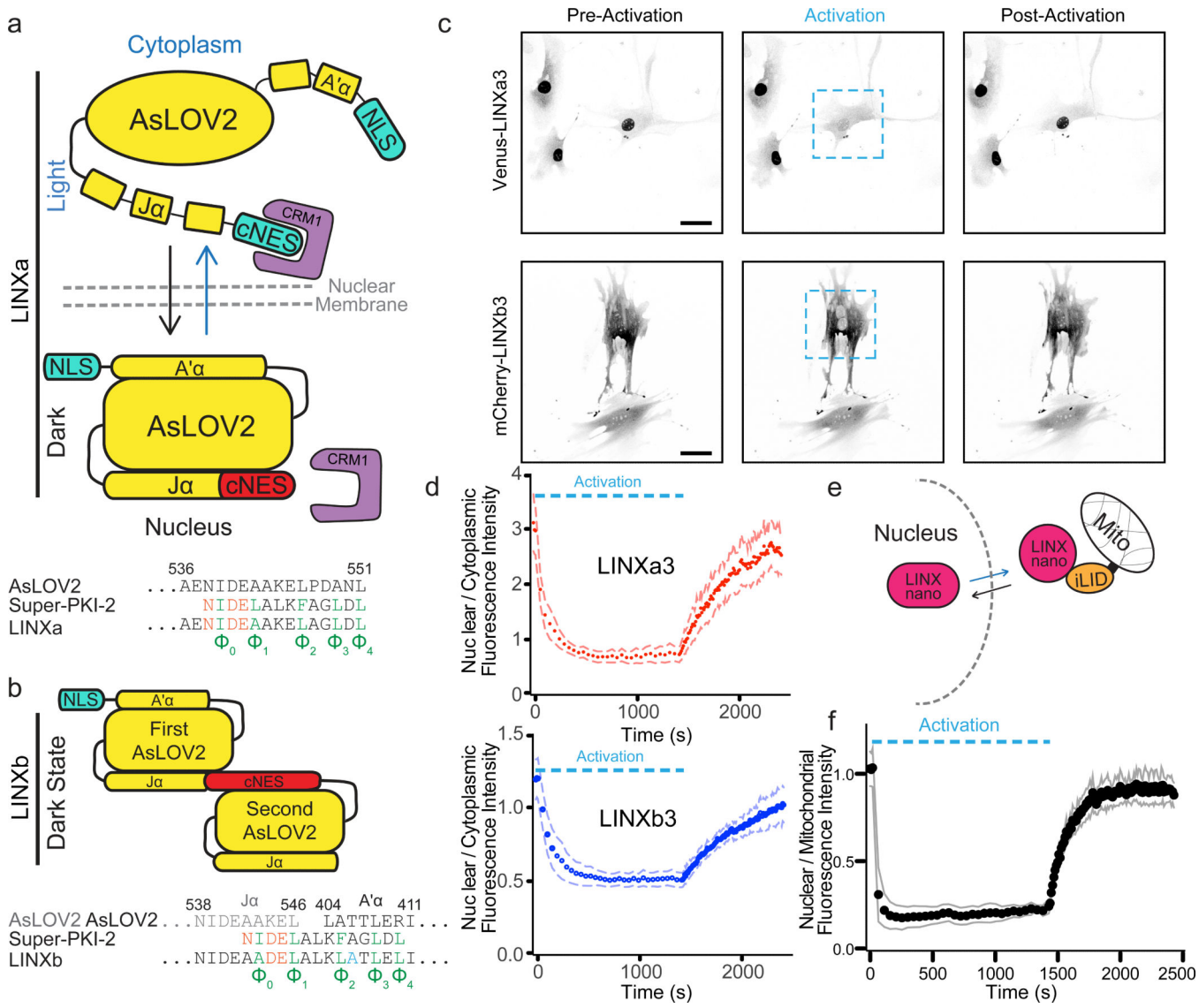

Figure 1.

Design of the Light Inducible Nuclear eXporter (LINX) and its use with the improved Light Inducible Dimer (iLID). (a) Design scheme for LINXa (cNES – conditional Nuclear Export Signal) illustrating its nuclear export upon binding to CRM1 after blue light illumination. Below the schematic the sequences for the WT Jα helix, the NES motif Super-PKI-2, and the engineered Jα helix in LINXa are shown. Residues important for nuclear export are shown in green. (b) Design scheme and sequences for LINXb. (c) Photoactivation of LINXa and LINXb fused to fluorescent proteins in mouse fibroblasts (IA32) (scale bar = 50 μm). Individual cells were activated in a field of cells, and nucleocytoplasmic ratios were measured as a function of time (Supplementary Movies 1 and 2 and Supplementary Fig. 3). (d) Quantification of nuclear/cytoplasmic fluorescence intensity change upon activation with blue light for LINXa3 and LINXb3. Mean values ± the standard error of the mean (s.e.m.) were calculated from images of multiple cells (LINXa3 n=5 and LINXb3 n=6). (e) LINX in combination with iLID enhances nuclear export and allows targeting to specific locations in

the cytoplasm. One half of the light inducible dimer (nano) was fused to LINX and the other half (iLID) to a mitochondrial anchor. (f) Quantification of photoactivation in IA32 cells using LINXa3-nano and iLID-Mito (n=3, mean ± s.e.m.).

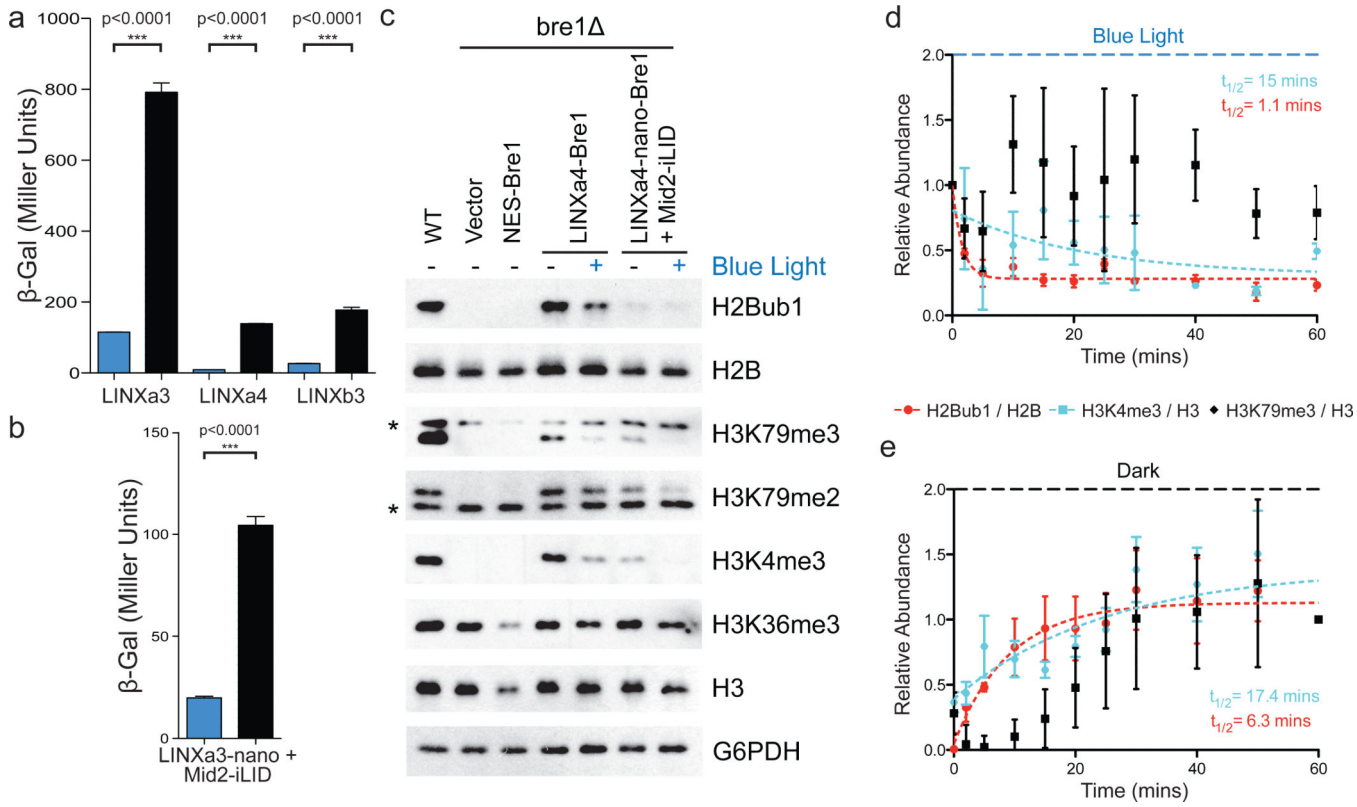

Figure 2.

Control of gene transcription and histone modifications with LINX. (a, b) β-Galactosidase activity in the light (blue bars) and dark (black bars) induced with LINX variants fused to a LexA DNA binding domain and the Gal4 activation domain (n=3, mean ± s.e.m., two-tailed t-test). (c) Light-mediated control of the Bre1 E3 ligase in a *BRE1* deletion strain as evidenced through immunoblotting with antibodies specific to various histone modifications (see Supplementary Fig. 12 for original film images). In all constructs the Bre1 NLS has been inactivated with mutations. Non-specific bands are indicated with asterisks. (d) Western blot quantification of histone modifications as a function of time after the transition from dark to blue light with the LINXa4-Bre1 switch (n=3, mean ± s.e.m. see Supplementary Fig. 11 and Supplementary Fig. 13 for original film images). (e) Western blot quantification of histone modifications as a function of time after the transition from blue light to dark with the LINXa4-Bre1 switch in (n=3, mean ± s.e.m. see Supplementary Fig. 11 and Supplementary Fig. 13 for original film images). Half-lives were determined from single exponential fits to the H2Bub1 and H3K4me3 relative abundance data using Prism 5.